Thermal analysis of TEFC induction motors

Conference Paper · November 2003

DOI: 10.1109/IAS.2003.1257630 · Source: IEEE Xplore

Aldo Boglietti
Politecnico di Torino

D. Staton
Motor Design Ltd

Thermal Analysis of TEFC Induction Motors

A. Boglietti*, A. Cavagnino*, D.A.Staton #

* Dip. Ingegneria Elettrica Industriale - Politecnico di Torino – C.so Duca degli Abruzzi, 24, 10129 Torino - ITALY
# Motor Design Ltd, 1 Eaton Court, Tetchill Ellesmere, Shropshire, UK

Abstract: **In order to manufacture smaller and more efficient electric motors an accurate prediction of the motor thermal performances at the design stage is a necessity. In addition, the thermal performance often needs to be analyzed when a motor is used in a different way to which it was originally designed for. An important example is the use of variable speed drives with induction motors designed for mains supply. These thermal requirements mean than accurate and reliable motor thermal models are required by the designers. In this paper the thermal behavior of Total Enclosed Fan Cooled (TEFC) induction motors are investigated using a commercially available software package called Motor-CAD®. This software has been used to develop thermal models for five industrial induction motors from the same series (rated powers of 4 kW – 7.5 kW – 15 kW – 30 kW – 55 kW, 4 poles, 380 V, 50 Hz). The models produced have been experimentally verified. In particular, for each motor, the results obtained using the software's default parameters have been compared with solutions obtained using tuned parameters obtained through thermal tests. The analysis and the results reported in the paper allow us to give some general guidelines useful for obtaining accurate thermal models of TEFC induction motors. In particular we give advice on developing models for use in the calculation of motor de-rating when changing from mains to inverter supplies.**

I. Introduction

In order to manufacture smaller and more efficient electric motors an accurate prediction of the motor thermal performances at the design stage is a necessity. In addition, the thermal performance often needs to be analyzed when a motor is used in a different way to which it was originally designed for. An important example is the use of variable speed drives with induction motors designed for mains supply. In such cases an accurate thermal model is required if the correct de-rating torque curve is to be calculated. Commercially available computer programs suitable for the thermal analysis of electric motors range from analytical to numerical finite element and Computational Fluid Dynamics (CFD) packages. In this paper the thermal behavior of Total Enclosed Fan Cooled (TEFC) induction motors are investigated using a commercially available software package called Motor-CAD® [1]. This software is based on an analytical lumped-circuit thermal model. The thermal network is based on resistors, power (current) sources and when the transient analysis is enabled a capacitance network is added. Resistances are used to model the main heat transfer paths within the machine, their value being dependent upon the dimension and the materials thermal conductivity. The motor loss contributions are modeled as the thermal equivalent to electrical current sources, i.e. power sources. The program and in particular the user interface is structured such that the users can easily input the electrical motor geometry and the complete lumped thermal network is automatically generated. All the heat transfer parameters are computed by the program, so the user need not be an expert in heat transfer analysis. Motor-CAD® has been used to develop thermal models for five industrial induction motors from the same series (rated powers of 4 kW – 7.5 kW – 15 kW – 30 kW – 55 kW, 4 poles, 380 V, 50 Hz see Fig. 1).

Fig. 1: TEFC motors used to generate test data.

The models produced have been experimentally verified. For each motor, the results obtained using the software's default parameters have been compared with solutions obtained using tuned parameters obtained using thermal tests. The analysis and the results reported in the paper allow us to give guidance as to what we believe to be the best approach to make best use of thermal software in electric motor design. In particular, the paper gives some general guidelines useful for obtaining accurate thermal models of TEFC induction motors. The resulting thermal models can help in the calculation of motor power derating when the machine supply is changed from the mains to an inverter.

II. TESTS AND EXPERIMENTAL DATA COLLECTION

The five induction motors have been thermally tested. The obtained data allow us to verify and set up the thermal models which will be described in the next sections. Measurements were made on the main motor temperatures, the motor losses and the cooling air speed. A short discussion of the thermal tests carried out is given below.

DC Thermal test

In this test the stator copper losses are present only. Series and parallel phase winding connections are used to supply the motor with a DC current equal to 50÷70% of the rated current. The cooling air speed is zero so a reduced current is necessary to avoid damage to the fan cooled motors. In the thermal steady state condition the adsorbed electrical power and the temperatures of the stator windings, stator core and external housing have been measured. The stator core and winding temperatures have been measured using a thermal sensor (PT100) positioned within the stator yoke and the end winding of each phase. The housing average temperature has been obtained by measuring the temperature at several external positions on the housing.

Variable frequency load tests

Steady state on-load thermal tests have been performed for supply frequency in the range 10 to 50 Hz. Measurements were made of the adsorbed electrical power, the mechanical power at the shaft and the temperatures of the stator windings, stator core and external housing. The motors have been regulated following the well know "V/f" law. For each supply frequency, the rated load torque has been defined as the torque that keeps the winding temperature equal to that measured during the load test at rated load and frequency (a tolerance of ±5°C has been considered). The different motor loss contributions have been calculated using motor loss separation based on the classical equivalent circuit approach.

Cooling air speed measurements

Measurements have been made of the air speed flowing in the open fin channels on the outside of the housing. Such tests were carried out under no-load conditions at the same frequencies as used in the AC load tests. The air speed has been measured using a digital anemometer at the beginning and at end of all the axial fin channels. Then the average values of the air speed at the extreme axial ends of the motor (fan and shaft ends) are calculated. In addition, a measurement of the axial air speed variation as function of the distance from the fan along a fin channel has been performed. For this measurement a lateral channel positioned in the middle of the housing has been chosen. As an example, Fig.2 and Fig. 3 show cooling air speed data for the 15 kW machine. Much more data relating to this cooling air speed analysis can be found in [4].

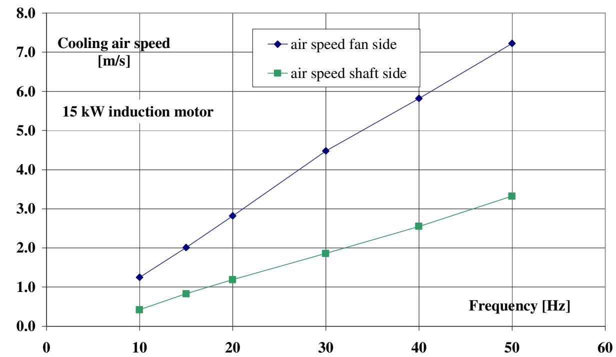

Fig. 2: Cooling air speed (fan and shaft side) versus. the fan speed.

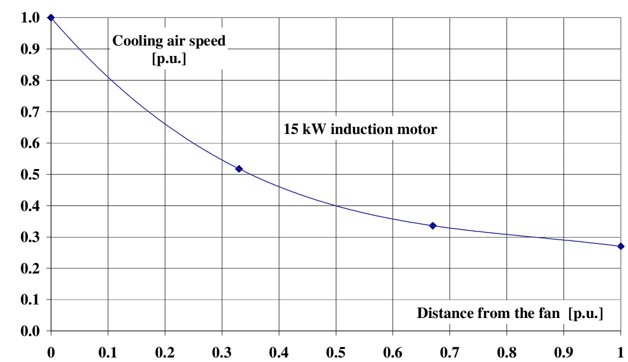

Fig. 3: Cooling air speed versus the distance from the fan.

The complexity of the cooling air speed is increased by the non uniform distribution of the air speed around the housing. In particular, the fan cowl supports do not allow a constant distribution of the air flow on the housing surface. The distribution for the motor running in counterclockwise direction is shown in Fig.4. When the motor is running in clockwise direction the air speed distribution has exactly the opposite circumferential distribution. This short discussion on the cooling air speed analysis highlights that the simulation of the cooling air speed in a thermal model is very complex and it does not have a simple solution.

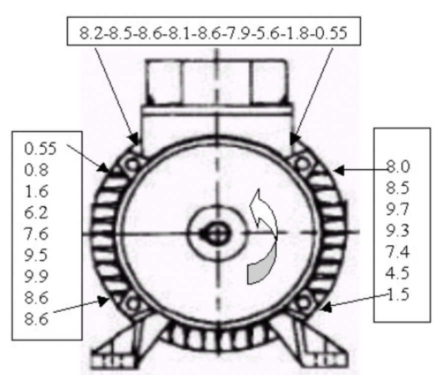

Fig. 4: Typical form of variation in fin channel air velocity with fin position, fan side, 4 kW motor (reported speed in m/s).

III. MOTOR THERMAL MODEL WITH DC SUPPLY

Using Motor-CAD® software, the previously described DC thermal tests have been simulated. The program require as input data the geometric dimensions of the motors, material properties and the value of the stator copper losses. Three type of model have been used:

Model 1: Convective and radiation heat transfer using default thermal model parameters provided by the program.
In this simulation the heat transfer by radiation has been taken into account even if the housing temperature does not reach a value so high to give any considerable radiation heat transfer. The default thermal parameters proposed by Motor-CAD® have been adopted.

Model 2: Convective heat transfer and default thermal model parameters provided by the program.
In this simulation the heat transfer by radiation has been neglected. Again, the default thermal parameters proposed by Motor-CAD® have been used.

Model 3: Convective heat transfer and tuned thermal model parameters.
In this simulation a selection of model parameters have been tuned until the computed temperatures match the measured ones. We have chosen the following three key parameters to calibrate the model:

- natural convection thermal resistance between housing and ambient;
- interface gap among the stator yoke and the housing;
- air thickness between the slot and the copper of the winding.

Fig. 5 shows interface gap data. The Motor-CAD® simulation values were obtained using a model set up to match measured and simulated iron and housing temperatures. Since the air gap between stator core and external frame is very small we can use a thermal resistance formulation for a simple rectangular structure (resistance proportional to length and inversely proportional to area) rather than the slightly more complex formulation for a hollow cylinder. As a consequence, the interface gap volume can be calculated from the product of the interface gap and the stator yoke external surface. The computed interface gap can be obtained by the following equation:

$$l_{gap} = R_{thgap} \, 2 \cdot \pi \cdot r_1 \cdot \lambda_{air} \cdot l \tag{1}$$

where:

λ_{air}	-	air conductivity
l	-	stator yoke length
r_1	-	stator yoke external radius
l_{gap}	-	interface gap

and:

$$R_{thgap} = \frac{\vartheta_{iron} - \vartheta_{housing}}{Losses} \tag{2}$$

where ϑ_{iron} and $\vartheta_{housing}$ are the stator iron and the housing temperatures respectively and Losses are the total losses produced by the dc supply.

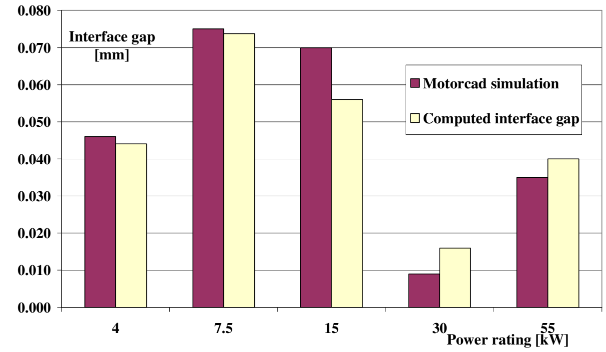

Fig.5: Interface gap comparison for the five motors.

Fig.6 compares predicted and measured natural convection housing to ambient thermal resistance values. The thermal resistance has been computed using the following equation:

$$R_{hous-amb} = \frac{\theta_{housing} - \theta_{amb}}{Losses} \tag{3}$$

where:

$R_{hous\text{-}amb}$	-	heat transfer thermal resistance
$\vartheta_{housing}$	-	housing temperature
ϑ_{amb}	-	ambient temperature

The results show a good agreement. This result confirms that the natural convection resistance between the housing and the ambient can be predicted with a high grade of accuracy [1] – even in this case where the housing outer geometry is very complex and not designed to optimize natural convection.

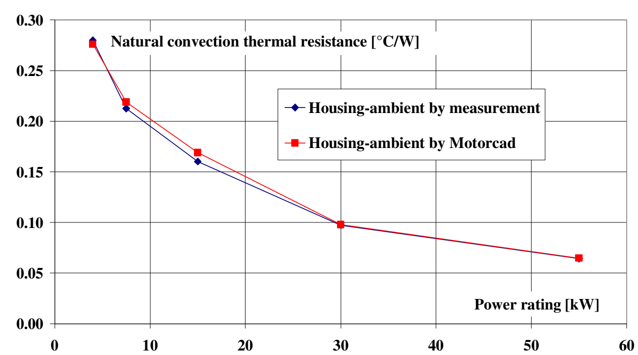

Fig.6: Housing natural convection resistance comparison.

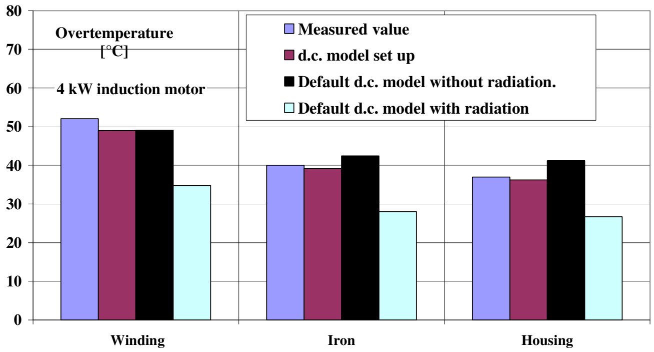

Fig. 7: Temperature comparison for the 4 kW motor.

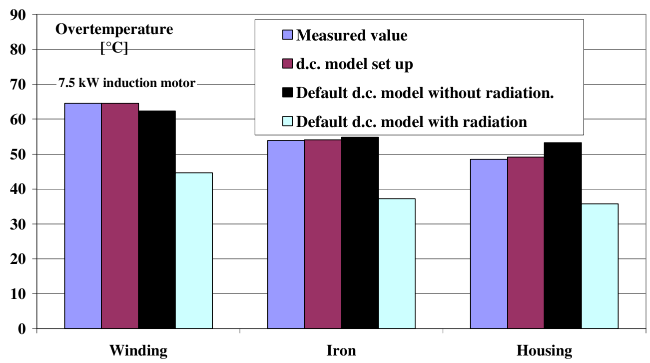

Fig. 8: Temperature comparison for the7.5 kW motor.

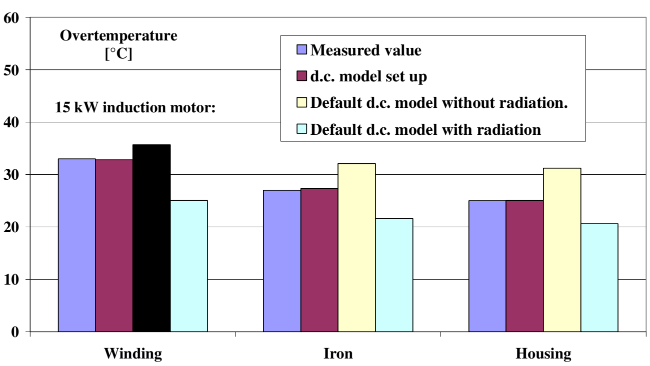

Fig. 9: Temperature comparison for the15 kW motor

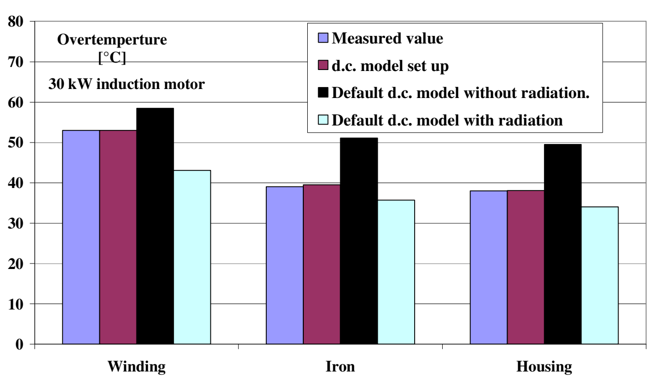

Fig. 10: Temperature comparison for the 30 kW motor.

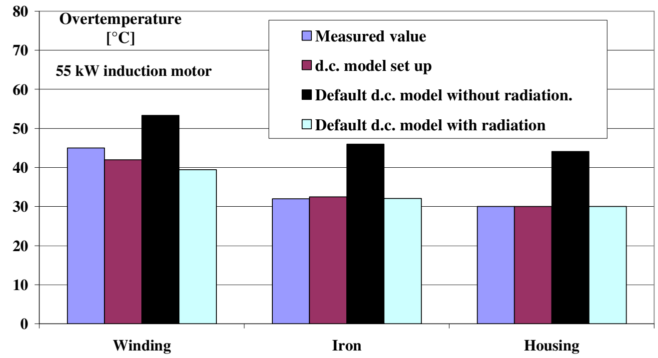

Fig. 11: Temperature comparison for the 55 kW motor.

Include Radiation in Lump Circuit Model

dT used in table below [degC]: 100

Component	Emissivity	View Factor	h
Units			
Housing [Active] - Fin Base	0.6	1	
Housing [Active] - Fin Sides	0.6	0	
Housing [Active] - Fin Tips	0.6	1	
Housing [Active] - Corner Cutout	0.6	1	
Housing [Front] - Fin Base	0.6	1	
Housing [Front] - Fin Sides	0.6	0	
Housing [Front] - Fin Tips	0.6	1	
Housing [Front] - Corner Cutout	0.6	1	
Housing [Rear] - Fin Base	0.6	1	
Housing [Rear] - Fin Sides	0.6	0	
Housing [Rear] - Fin Tips	0.6	1	
Housing [Rear] - Corner Cutout	0.6	1	
Endcap [Front] - Radial Area	0.6	1	
Endcap [Front] - Axial Area	0.6	1	
Endcap [Rear] - Radial Area	0.8	1	

Fig.12: Motor-CAD® Emissivity and View Factor table.

The temperatures comparison obtained using the three models and measurements are shown in Fig.7 to Fig.11 (one graph for each of the five motors). In each graph the winding, iron and housing temperatures are reported. The five graphs show good results for Models 2 and 3. In particular, Model 3 (obtained using parameters set up using the DC test) shows an excellent agreement between the predicted and the measured temperatures. Model 1 (model with thermal radiation included) is the worst one with a consistent discrepancy between the measured and the predicted temperatures. The predicted temperatures are lower than the measured ones. One avenue of research that is currently underway is to investigate the amount of dissipation through the feet to test bed as it may well be this that makes it necessary to neglect radiation to obtain good agreement with test, i.e. the dissipation to the test is included in the model but may not be a significant cooling mechanism in this particular case.

The results obtained using Model 2 seem to indicate that the calculation of natural convection heat transfer within the program is over optimistic. Conversely, Fig 6 seems to indicate that natural convection is accurately calculated.

Again, the problem is likely to be due to dissipation to the base plate being different in the model to that in reality and is being investigated further.

In Model 2 we have neglected radiation completely. A more realistic model would to select a value of emissivity that matches that of the paint used on the outside of the motor, i.e. set emissivity values for surfaces shown in Fig.12. The problem is that it is often difficult to obtain such data as manufactures of induction motors do not usually try to optimize the radiation component as they have a relatively good cooling mechanism in the forced convection from the fan, i.e. unknown emissivity value for the paint used. Conversely, in naturally convected servo motors radiation can form a significant proportion of the total dissipation and the motor manufacturer will usually know an emissivity value for the paint used.

IV. Motor Thermal Model With AC Supply

As shown in the previous section, Model 3 is able to predict the temperatures with good agreement. This DC model has been chosen as starting point from which thermal models have been developed that take into account the air speed and the motor loss distribution variations for running load conditions. In order to gain information on the thermal behavior during the normal operation, the five induction motors have been tested under load with inverter supply using fundamental frequencies from 10 Hz up to 50 Hz. Starting from the model set up with the DC supply, loss distribution, shaft and cooling air speed values for the different frequencies have been introduced into the model data. It is important to remark that when the induction motor rotates the fan provide an additional air flow orthogonal to the fluid motion due to natural convection. In this analysis, the main problem is to predict the forced convection heat transfer coefficient. The software calculates the forced convection heat transfer coefficient using well know dimensionless heat transfer correlations. These are based on the housing geometry length, fluid material properties (air) and the air velocity [1]. This is then combined with the natural convection heat transfer coefficient to form the mixed convection heat transfer coefficient [4]. For this analysis step two AC models have been developed:

AC Model 1: In this model the local air velocity has been changed to match the cooling air speed values provided by the experimental tests for each motor supply frequency.

AC Model 2: In this model the software's default estimates for local air velocity reduction with distance from the fan has been used. The defaults data provided by Motor-CAD® are just estimates from previous published data. In addition, it is important to underline that they can vary in different fin/cowlings/fan designs and so should be calibrated for a given type of design.

In the AC Model 1 the cooling air speed on the fan output has been considered as the average value of the several air speed measured all around the fan cowl (see Fig.4). The reduction of the air speed along the axial direction of the housing (see Fig. 3) has been taken into account by changing the local air velocity multiplier [pu] as provided in the table editor provided by Motor-CAD® (see Fig.13).

Constant Speed Fan (Blower Unit) — Input Flow Rate or Velocity: Velocity
Default RPM: 600 — Default Flow Rate @Default RPM: 0.0541
Shaft Speed [rpm]: 542 — Default Velocity @Default RPM: 2.82

Component	Input h?	Forced Convection Correlation	h[input] or h[adjust]	Air Velocity	Air Velocity	hnc @ dT=100.0C	hf dT
Units			W/m2/C	pu	m/s	W/m2/C	W/
Housing [Active]- Fin Base		Fin Channel	1	0.75	1.911	5.05	1
Housing [Active]- Fin Sides		Fin Channel	1	0.75	1.911	5.05	1
Housing [Active]- Fin Tips		Flat Plate	1	0.75	1.911	7.79	6
Housing [Active]- Corner Cutout		Fin Channel	1	0.75	1.911	5.769	1
Housing [Front]- Fin Base		Fin Channel	1	0.31	0.7897	5.05	5
Housing [Front]- Fin Sides		Fin Channel	1	0.31	0.7897	5.05	5
Housing [Front]- Fin Tips		Flat Plate	1	0.31	0.7897	7.79	2
Housing [Front]- Corner Cutout		Fin Channel	1	0.31	0.7897	5.769	5
Housing [Rear]- Fin Base		Fin Channel	1	1	2.547	5.05	2
Housing [Rear]- Fin Sides		Fin Channel	1	1	2.547	5.05	2
Housing [Rear]- Fin Tips		Flat Plate	1	1	2.547	7.79	1
Housing [Rear]- Corner Cutout		Fin Channel	1	1	2.547	5.769	2
Endcap [Front] - Radial Area		Flat Plate	1	0.5	1.274	8.017	3

Fig. 13: Motor-CAD® air speed coefficient table

V. Result Analysis

The following graphs show measured and predicted motor winding, iron and housing temperatures for the five motors as a function of the supply frequency. For all measured points a bar showing the ±5°C variation has been drawn. This bar has been considered as the error tolerance expected on the predicted temperature. The motor tests have been performed to define the torque derating for a TEFC induction motor when it is employed in a variable speed drive, i.e. in a TEFC induction motor the cooling effects are strongly depending on the rotational speed. As a consequence, during the load tests, the motor torque has been reduced with the supply frequency until the steady state winding temperature was equal to the temperature measured at rated frequency of 50 Hz. The measured temperatures have been used as reference in thermal simulation.

From the comparison between predicted and measured temperatures it is possible to make the following remarks:

- AC Model 2, which is based on the default forced convection adjustment coefficient, has lower accuracy than AC Model 1.

- Both models are more accurate at higher speeds.

--- Winding temperatures ---

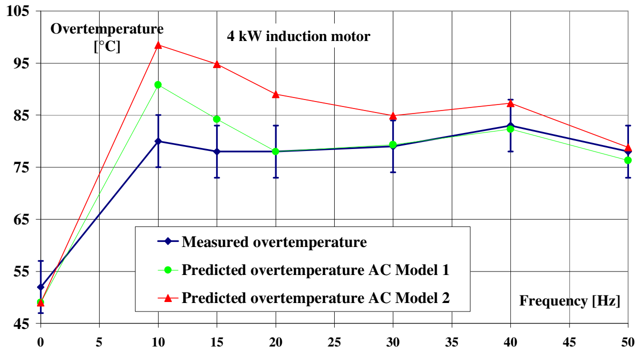

Fig. 14: Winding temperature comparison for 4 kW motor

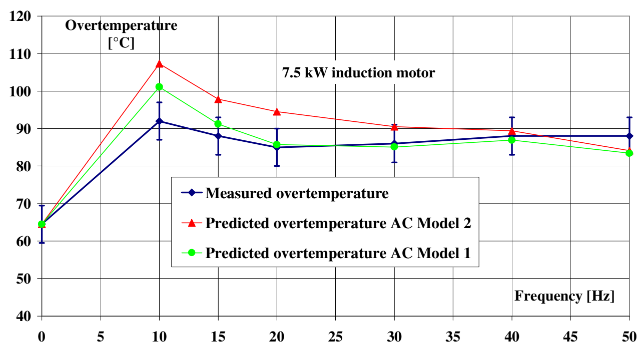

Fig. 15: Winding temperature comparison for 7.5 kW motor

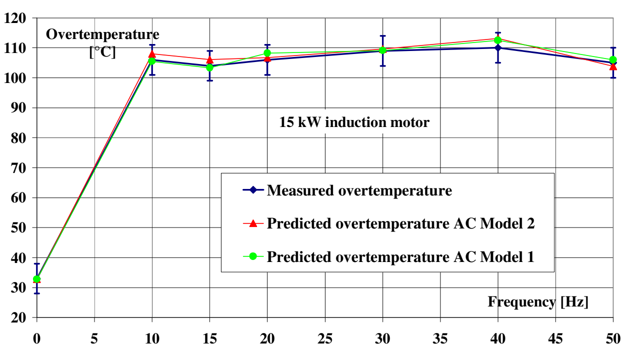

Fig. 16: Winding temperature comparison for 15 kW motor

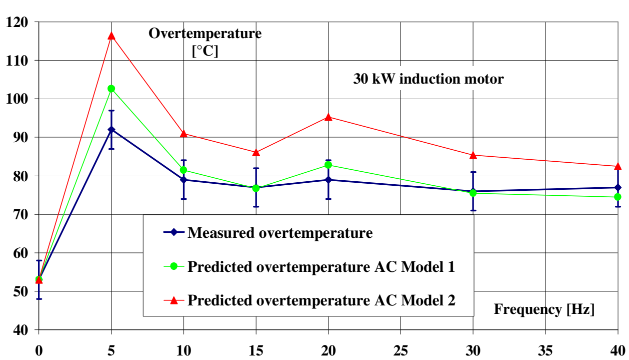

Fig. 17: Winding temperature comparison for 30 kW motor

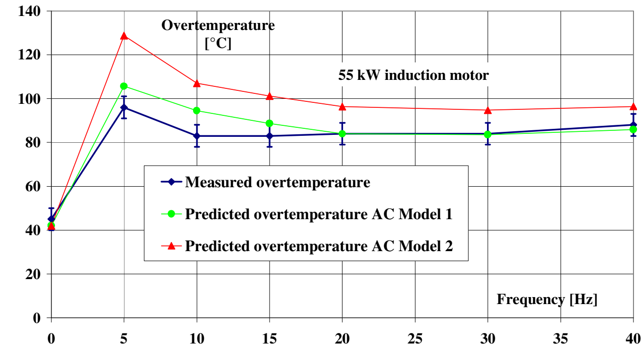

Fig. 18: Winding temperature comparison for 50 kW motor

--- Iron temperatures ---

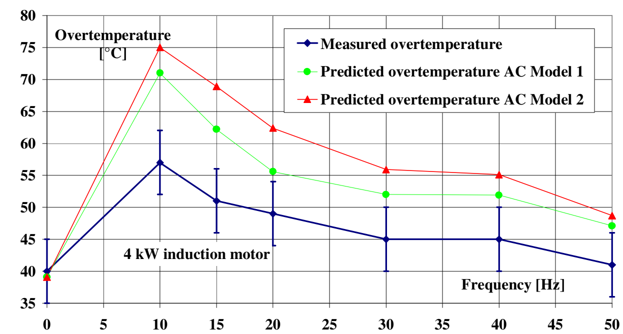

Fig. 19: Iron temperature comparison for 4 kW motor

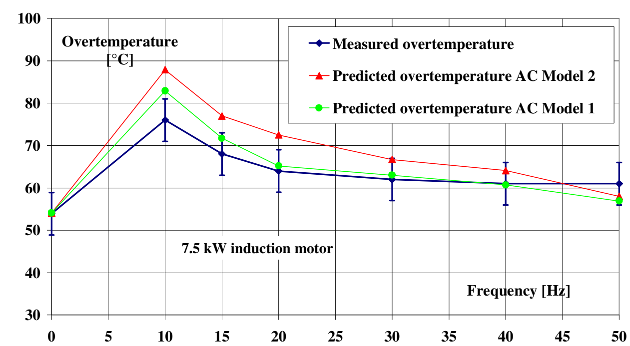

Fig. 20: Iron temperature comparison for 7.5 kW motor

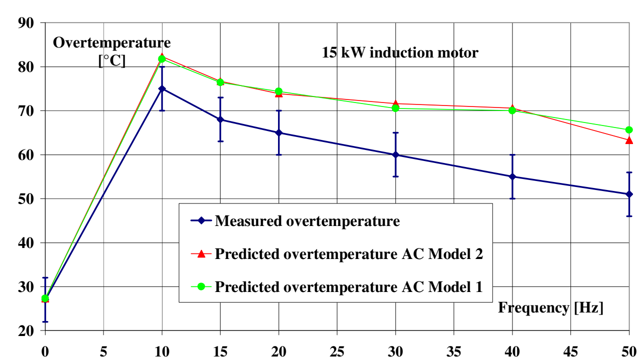

Fig. 20: Iron temperature comparison for 15 kW motor

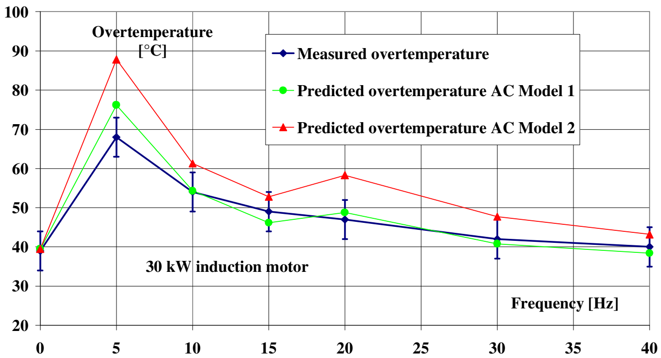

Fig. 21: Iron temperature comparison for 30 kW motor

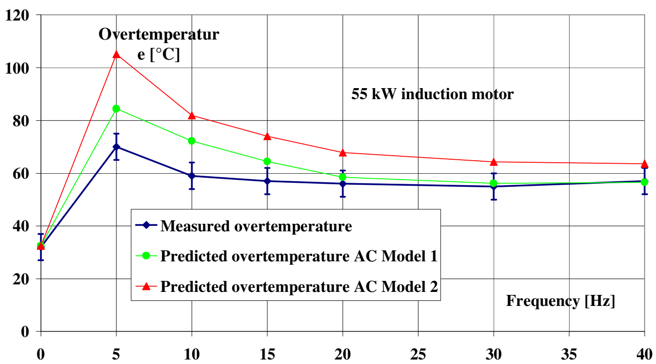

Fig. 22: Iron temperature comparison for 55 kW motor

--- Housing temperatures ---

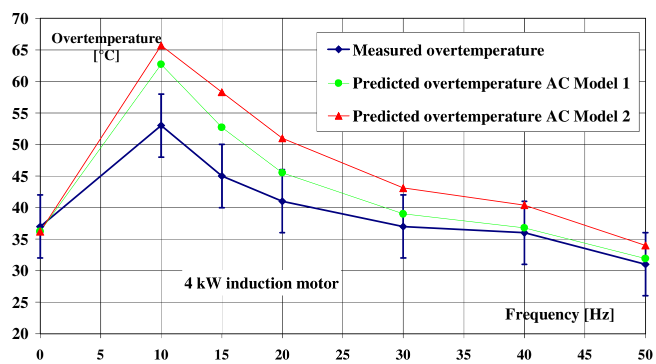

Fig. 23: Housing temperature comparison for 4 kW motor

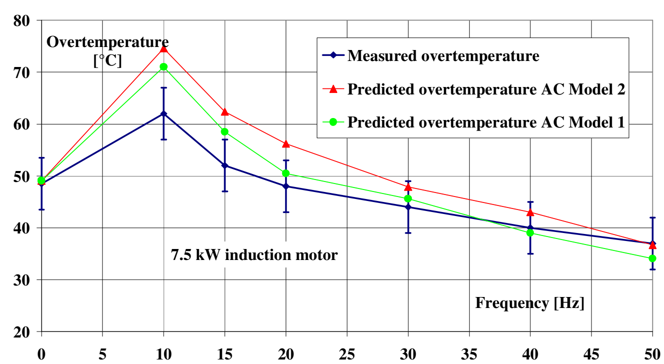

Fig. 24: Housing temperature comparison for 7.5 kW motor

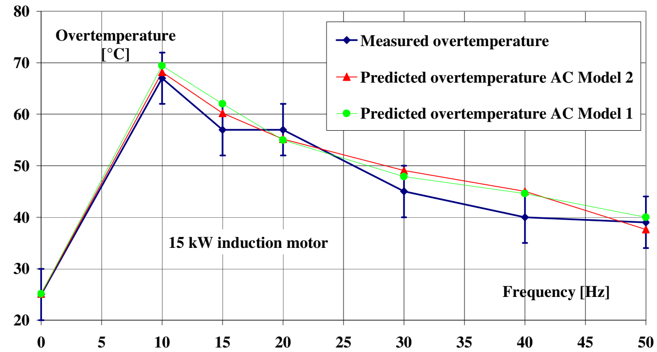

Fig. 25: Housing temperature comparison for 15 kW motor

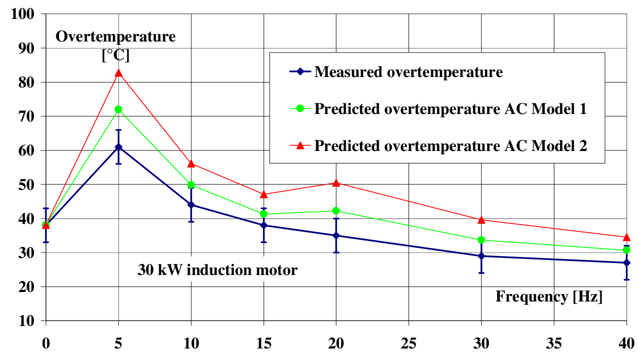

Fig. 26: Housing temperature comparison for 30 kW motor

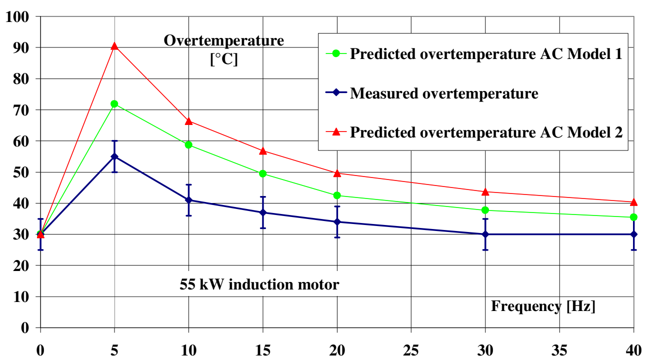

Fig. 27: Housing temperature comparison for 55 kW motor

This tends to reinforce the fact that neglecting radiation may be in error and that the unknown cooling to the test bed will have more impact on the simulation results at low speeds. In addition the measurements of low air speed is particularly delicate and such errors will effect the accuracy of the AC Model 1.

- Windings temperatures calculated by AC Model 1 for frequencies larger than 10 Hz are within the desired ± 5 °C measurement band.

- The accuracy of the iron temperature prediction is worse than that for the winding. This is not too bad an outcome as the winding is a more critical component in terms of motor life.

- Both models give overestimates of the temperatures. As a consequence, the use of these results can be considered as a safe choice by the users.

The following final remarks on the development and use of thermal models can be made. The development of accurate thermal models is more difficult than equivalent electromagnetic analysis. For instance, in the case of electromagnetic finite element analysis you expect a relatively accurate model if you have a good knowledge of the geometry and material properties. The development of accurate thermal models depend heavily on the prediction of key manufacturing deficiency parameters such as interface gaps and impregnation goodness. Such parameters are difficult to physically measure and they are best estimated by model calibration using experimental data. Thermal models based on sophisticated 3D numerical analysis programs involving CFD allow us to make better predictions of some thermal performance data such as convection heat transfer coefficients. However, CFD does not help with the prediction of the manufacturing deficiency parameters. In some respects such parameters are more difficult to analyze using numerical analysis. Also, CFD is expensive and time consuming and in not in general use for industrial motor design.

VI. Conclusions

In the paper a deep thermal analysis on a set of five TEFC induction motors have been discussed. Some of the main problems to be solved in thermal simulations have been analyzed and discussed. The work has put in evidence that a superficial knowledge of the geometrical and material properties used in electrical machines construction is not sufficient to give an accurate prediction of the thermal performance. This is because many of the complex thermal phenomena that occur in electric machines cannot be solved by pure mathematical means. In particular, for TEFC induction motors, the air speed value is a sensitive quantity. As a consequence, it is important that the air speed adopted in the model has to be selected between the lower and the higher measured ones. In fact, the choice of the minimum value corresponds to a safer temperature prediction. Different solutions can be proposed for solving these problems. As an example, taking into account that for most companies electrical thermal rating tests represent a must for defining the rated values, a data base of thermal parameters can be developed. In this way, it is possible to create curve fitting analytical equations that can be used when predicting the key thermal quantities of future new motors. As reported in the paper an accuracy of ±5 °C on the winding temperature can be obtained and it can be considered an excellent target for most applications.

Some of the discrepancies found in this paper may be due to neglecting radiation due to the lack of emissivity data for the paint used (radiation can easily be turned off in the model). This is complicated by the fact that there is an unknown amount of dissipation via conduction through the motor feet to the test bed. In the analysis we have included a model for the test bed dissipation, but in practice this model has not been calibrated and may be inaccurate. This aspect is being investigated further. Also, more testing, analysis and algorithm development is currently underway and will form the basis of a future technical paper in which we hope to obtain even better agreement than found in this paper with less effort required in terms of calibration effort by software user, i.e. a database of expected parameters such as interface gaps and impregnation goodness for different manufacturing techniques is being developed and is being built into the software.

Thermal models are also very useful even in cases where the designer does not have a finely tuned calibrated model that gives good absolute accuracy. In such cases the designer can vary design variables such as the impregnation material and its goodness, motor dimensions and losses (iterative process with electromagnetic design) and see how these effect the temperatures in the machine. Even if the absolute temperatures predictions may be in error, the percentage temperature change for a given design change will usually be a correct reflection of reality and will help in the motors optimization.

Acknowledgment

The authors thank Dr. Enrico Galaverna for his activity developed for Laurea Thesis at the Politecnico di Torino, and the FIMET Motori & Riduttori for the technological support to this research.

References

[1] D. Staton, “Thermal analysis of electric motors and generators”, Tutorial course, IEEE IAS Annual Meeting 2001, Chicago, USA.
[2] D. Staton, “Motor-CAD Tutorial”, on line help of the Motor-Cad® software, 2001.
[3] P.Mellor, D.Roberts, D. Turner, “Lumped parameter thermal model for electrical machines of TEFC design”, IEE Procedings, Vol. 138, September 1991.
[4] D. Staton, A. Boglietti, A. Cavagnino, “Solving the More Difficult Aspects of Electric Motor Thermal Analysis”, IEMDC 2003 Conference Proc. 1-4 June 2003, Madison Wisconsin, USA.